Electronic Structure and Bonding in Cerium (Nitride) Compounds: Trivalent versus Tetravalent Cerium

Gregory A. Landrum,[a] Richard Dronskowski,*[a] Rainer Niewa,[b] and Francis J. DiSalvo[b]

Abstract: The assignment of the cerium oxidation state in the recently prepared and structurally characterized Ce_2MnN_3 phase is problematic. Based upon E^0 values from aqueous solution, one would suggest the crystal composition to be $(Ce^{3+})_2Mn^{3+}(N^{3-})_3$. The experimental data, however, indicate that Ce_2MnN_3 is nonmagnetic; this alludes to (but does not prove) a cerium oxidation state of +4, giving $(Ce^{4+})_2Mn^{+}(N^{3-})_3$. Previous theoretical work supports the latter oxidation state assignment. Here we carry out a systematic theoretical examination (using the TB-LMTO-ASA method) of the electronic structures of a number of Ce compounds, in which the oxidation state on Ce is more easily assigned. The Ce^{3+} compounds examined are CeF_3, $CeCl_3$, $CeBr_3$, and CeN. Our Ce^{4+} data set includes CeC, CeO_2, Li_2CeN_2, and Li_2CeP_2. CeN, which is nonmagnetic despite the fact that it contains Ce^{3+}, makes it clear that the absence of a magnetic moment in a compound does not necessarily preclude the presence of Ce^{3+}. Our calculations indicate that the remaining Ce-centered electron in CeN has substantial d character and is delocalized to form a partial Ce–Ce bond instead of being highly localized in Ce-centered f states, like the unpaired electron in $CeBr_3$. Careful inspection of the band structures of these compounds shows some qualitative trends that may be useful in assigning oxidation states: in Ce^{3+} compounds there is at least one occupied band that is clearly made up mostly of Ce states, while in systems with Ce^{4+}, the small Ce contributions are delocalized across many occupied bands. Using this criterion, we conclude that $(Ce^{4+})_2Mn^{+}(N^{3-})_3$ is the correct oxidation state assignment for Ce_2MnN_3. We suspect that the high oxidation state on Ce is stabilized by the large number of N^{3-} ions surrounding it in the crystal.

Keywords: cerium · density functional calculations · nitrides · oxidation state · solid-state chemistry

Introduction

The assignment of oxidation states is a formal (classical) approach used to roughly characterize chemical bonding in new compounds. Thus, some specific training is a prerequisite and needs to be based upon the competent knowledge of a particular class of materials. When this experimental database is too small, the question arises whether electronic-structure calculations may help in the assignment. The question is far from being trivial, since the oxidation states (or formal charges) are typically far larger than those observed from quantum mechanical calculations, particularly for higher oxidation states. In addition, any quantum mechanical prescription for calculating atomic charges unavoidably contains some degree of arbitrariness.

The synthesis and structure of Ce_2MnN_3 was recently reported by one of us.[1] Accompanying the structure was an analysis of the bonding in the MnN_3 sublattice of Ce_2MnN_3 based upon extended Hückel theory. The Ce oxidation state was assumed to be +4 based upon calculated charges from a first-principles calculation. The presence of Ce^{4+} in the structure gives rise to $(Ce^{4+})_2Mn^{+}(N^{3-})_3$ as the chemical formulation in the crystal. Here Mn has an oxidation state of +1, which seems counter-intuitive, at best. Since E^0 values in aqueous solution indicate that Mn^{2+} is capable of reducing Ce^{4+} to Ce^{3+}, we would certainly not expect to find Ce^{4+} in the presence of Mn^{+}. A more likely formulation is: $(Ce^{3+})_2Mn^{3+}(N^{3-})_3$. Since CeN, which also contains Ce^{3+}, is nonmagnetic,[2] magnetic measurements do not allow us to distinguish between the two formulations.

In this contribution, we present an analysis of density functional calculations on a number of compounds containing Ce^{3+} or Ce^{4+}. Our goal in this analysis is twofold. Primarily we

[a] Prof. R. Dronskowski, Dr. G. A. Landrum
Institut für Anorganische Chemie
Rheinisch-Westfälische Technische Hochschule
Prof.-Pirlet-Str. 1, D-52074 Aachen (Germany)
Fax: (+49) 241-8888-288
E-mail: drons@HAL9000.ac.rwth-aachen.de

[b] Dr. R. Niewa, Prof. F. J. DiSalvo
Department of Chemistry, Cornell University
Ithaca, New York, 14853-1301 (USA)

  0947-6539/99/0502-0515 $ 17.50+.50/0

would like to determine the oxidation states in Ce_2MnN_3. We also hope, through a systematic examination of a number of compounds, to develop a feeling for the signposts in the electronic structure pointing to Ce^{3+} or Ce^{4+}.

Computational Methodology

Electronic structure calculations were performed by means of ab initio all-electron techniques with scalar-relativistic corrections to account for heavy-atom properties. The specific method used was Linear Muffin-Tin Orbital (LMTO) theory[3–6] which, in a nutshell, represents a fast, linearized form of the KKR method.[7, 8] It accounts for the potential from all the electrons and is applicable to materials composed of atoms from any part of the periodic table. The almost minimal, unfixed LMTO basis sets adjust dynamically to the respective potentials.

The electronic energy was calculated by density-functional theory, replacing the many-particle problem by the self-consistent solution of the Kohn–Sham equations,[9, 10] parametrized according to von Barth and Hedin.[11] Diagonalization and integration of the scalar-relativistic Hamiltonian in reciprocal space was performed with the help of an improved tetrahedron method.[12] All calculations were checked for convergence of energies and orbital moments with respect to the number of k points. The basis set of short-ranged[13] atom-centered TB-LMTOs contained s-f valence functions for Ce and s-d valence functions for all other atoms (higher energy valence functions were included with a downfolding technique). When necessary, empty spheres (atomic wave functions without nuclei) were incorporated in order to increase variational freedom and improve packing. Starting from atomic Hartree potentials, the structure was then iterated by use of the atomic-spheres approximation (ASA), by employing muffin-tin spheres blown up to overlapping and volume-filling spheres. The locations of the empty spheres, as well as the ASA radii, were determined by means of an automated procedure based upon the Hartree sizes of the atoms. In all cases, the structures used for the calculations were those determined experimentally. After having reached self-consistency, charge-density plots were generated by dropping any shape approximations for the potential inside the crystal. The program used was TB-LMTO 4.7,[14] run under AIX 4.2 on an IBM RS/6000 43P.

The bonding in the crystal structures under study was examined within the framework of crystal orbital Hamilton population (COHP) analysis.[15] This technique provides information analogous to the familiar crystal orbital overlap population (COOP) analysis[16] used in extended Hückel calculations. [17] While COOP curves are energy-resolved plots of the Mulliken overlap population between two atoms or orbitals, a COHP curve is an energy-resolved plot of the contribution of a given bond to the bonding energy of a system. There is one very important difference between COHP and COOP curves: while COOPs are usually presented as an *average* of several bonds, COHPs typically include the *sum* of those bonds. While this does not affect the shape of COHP curves, it does change their size. All COHP curves are presented here in a format similar to COOP curves: positive values are bonding, and negative antibonding (i.e., we have plotted $-$COHP instead of COHP).

Abstract in German:

Die Angabe einer Oxydationszahl für das Ceratom in der erst kürzlich präparierten und strukturell umfassend beschriebenen Verbindung Ce_2MnN_3 bereitet erhebliche Schwierigkeiten. Anhand von in wäßriger Lösung bestimmten Normalpotentialen läge die kristallchemische Formulierung $(Ce^{3+})_2Mn^{3+}(N^{3-})_3$ nahe, gleichwohl erweisen die experimentellen Befunde Ce_2MnN_3 als unmagnetisch; dies deutet im Sinne von $(Ce^{4+})_2Mn^{+}(N^{3-})_3$ auf vierwertiges Cer hin, ohne den Sachverhalt jedoch unumstößlich beweisen zu können. Allerdings untermauern bisherige theoretische Beiträge die letztere Oxydationszahl.

Wir berichten an dieser Stelle über systematische theoretische Untersuchungen mit Hilfe des TB-LMTO-ASA-Verfahrens hinsichtlich der elektronentheoretischen Strukturen einer ganzen Reihe von Cerverbindungen, in denen die Wertigkeiten des Cer offensichtlich sind. Die Phasen mit dreiwertigem Cer umfassen CeF_3, $CeCl_3$, $CeBr_3$ und CeN, diejenigen mit vierwertigem Cer dagegen CeC, CeO_2, Li_2CeN_2 und Li_2CeP_2.

Die Verbindung CeN mit dreiwertigem Cer offenbart, daß die Abwesenheit eines magnetischen Moments nicht notwendigerweise die Anwesenheit von Ce^{3+} ausschließt. Unsere Berechnungen belegen vielmehr, daß das verbleibende Ce-zentrierte Elektron erheblichen *d*-Charakter aufweist und in Form einer Ce–Ce-Teilbindung delokalisiert ist; im Gegensatz dazu ist das ungepaarte Elektron des $CeBr_3$ in Ce-zentrierten *f*-Zuständen hochgradig lokalisiert.

Die sorgsame Untersuchung der elektronischen Bandstrukturen all dieser Verbindungen liefert einige qualitative Anzeichen, die bei der Zuordnung von Oxydationszahlen dienlich sein können: in Verbindungen mit Ce^{3+} existiert wenigstens ein besetztes Band, welches nahezu vollständig aus Ce-Elektronenbahnen aufgebaut wird. Dagegen sind die Ce-Beiträge in Verbindungen mit Ce^{4+} über viele besetzte Bänder delokalisiert. Anhand dieses Merkmals schließen wir, daß $(Ce^{4+})_2Mn^{+}(N^{3-})_3$ die korrekte Zuordnung der Oxydationsstufen ist. Weiterhin unterbreiten wir, daß die hohe Wertigkeit des Cer im Kristall durch die große Anzahl koordinierender N^{3-}-Ionen hervorgerufen wird.

Results and Discussion

Trivalent cerium: We begin our discussion by examining some systems which clearly contain Ce^{3+}: CeF_3, $CeCl_3$, and $CeBr_3$. We will look at $CeBr_3$ in some detail, then briefly summarize the results for $CeCl_3$ and CeF_3.

The structure of $CeBr_3$, shown in Figure 1 contains chains of Ce-centered face-sharing trigonal prisms running along the *c* axis.[18] Neighboring chains are shifted by one half of the *c* lattice constant in such a way that the rectangular faces of each trigonal prism are capped by Br atoms from neighboring chains. The Ce–Br distances within each chain (3.11 Å) and

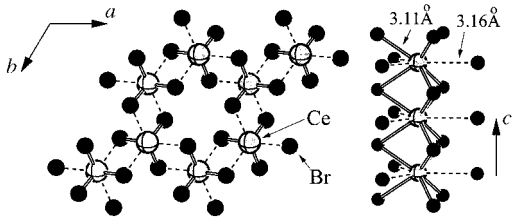

Figure 1. Left: A view of the structure of $CeBr_3$ down the *c* axis. Right: One chain of trigonal prisms emphasizing the Ce coordination environment.

those between chains (3.16 Å) are quite similar to each other; the Ce^{3+} ion is nine-coordinate. The closest Ce–Ce contacts, along the chains of trigonal prisms, are quite long: 4.44 Å. Since this is significantly longer than twice the Ce^{3+} effective ionic radius for ninefold coordination (2.39 Å),[19, 20] we do not expect significant Ce–Ce interactions here.

The Ce^{3+} valence electron configuration in $CeBr_3$ formally should be $(4f)^1(5d)^0(6s)^0(6p)^0$. With one electron in the 4f shell, we would predict that $CeBr_3$ should be magnetic. A spin-polarized calculation (in which the numbers of α, or spin-up, and β, or spin-down, electrons are allowed to be different) of the electronic structure of $CeBr_3$ fits our expectations neatly, predicting one unpaired electron per Ce^{3+} ion in $CeBr_3$. The spin-polarized density of states (DOS) of $CeBr_3$ is shown in Figure 2. While the α and β DOS curves differ very little in the region of occupied (bromine 4p-centered) states between 2 and 6 eV below the Fermi level (ε_F), there are large differences in the immediate vicinity of ε_F. The Fermi level lies

0947-6539/99/0502-0516 $ 17.50+.50/0 *Chem. Eur. J.* **1999**, *5*, No. 2

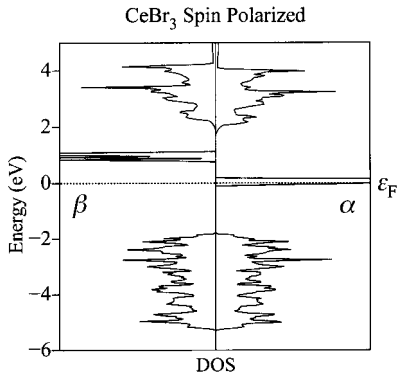

Figure 2. The spin-polarized density of states (DOS) calculated for $CeBr_3$. The right and left sides show the DOS for the α and β spins, respectively. The DOS curve has been shifted so that ε_F (indicated with a horizontal dotted line) lies at 0 eV.

close to the bottom of a sharp peak in the α states, while the corresponding β states lie about 1 eV higher in energy. The broader set of unoccupied states lying between 2 and 4 eV above ε_F are similar in shape for the α and β spins, but the β states are slightly (about 0.1 eV) higher in energy.

Figure 3 shows two fatband plots for the α spins of $CeBr_3$. These fatband plots are the band structure equivalents of projected DOS plots: not only are the band structures shown, but the widths of the lines are proportional to the contribution of a given set of atomic orbitals to the crystal orbitals. From

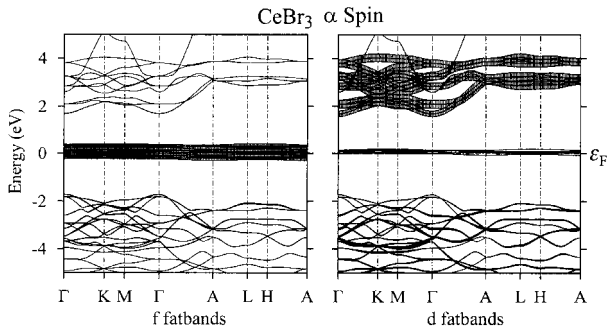

Figure 3. Fatband plots for the α spins of $CeBr_3$. The widths of the lines are proportional to the contribution of the Ce 4f (left plot) or Ce 5d (right plot) atomic orbitals to the crystal orbitals. The bands are shifted so that ε_F (indicated with a horizontal dotted line) lies at 0 eV.

these plots it is clear that the major contributors to the α states directly in the vicinity of ε_F are the Ce 4f orbitals. These orbitals are very localized in energy, appearing almost entirely in one small group of bands. On the other hand, while the Ce 5d orbitals show their largest contributions to the unoccupied bands between 2 and 4 eV, they are also mixed to a small amount into the occupied bands below -2 eV. This is perhaps difficult to see in the fatband plot at the right of Figure 3, but can be seen more clearly in a projected DOS plot for the Ce 5d orbitals (shown below in Figure 4).

The narrowness of the Ce 4f bands in Figure 3, as well as the narrow peaks in the spin-polarized DOS curve of Figure 2, tell us that these states are quite localized on the Ce atoms. If these levels were involved in significant interactions either between the Ce atoms or with bromines, we would expect to see considerably more band width. This fits in well with our general expectation that the 4f orbitals on the lanthanides tend to be very contracted: they have little spatial extent.

Figure 4 shows projected DOS and COHP curves for $CeBr_3$. For both the DOS and COHP curves the sums of the contributions from α and β spins are shown, as can be seen from the double peak in the region between 0 and 2 eV. As we

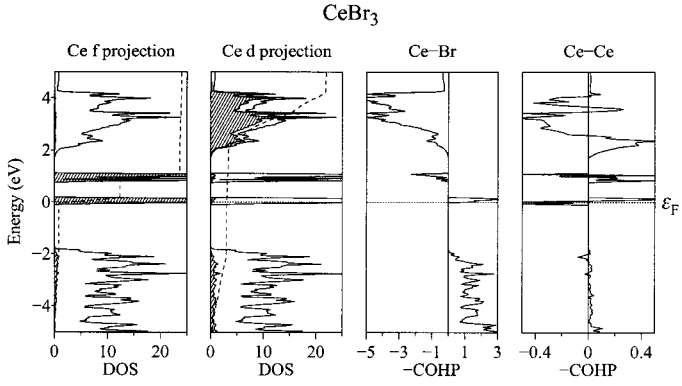

Figure 4. Total DOS, Ce 4f and 5d projected DOSs, and COHP curves for the Ce–Br and Ce–Ce interactions in $CeBr_3$. The dashed line in each DOS curve shows the integration of the projected states. To make the projected DOS curves more visible, the DOS is magnified. The Ce–Br COHP includes the sum of all nine close Ce–Br contacts, while the Ce–Ce curve is the sum of the two Ce–Ce contacts along the chains. All curves are shifted so that ε_F (the horizontal dotted line) lies at 0 eV.

saw in the band structure, the peaks in the DOS at ε_F (from the α spins) and about 1 eV (from the β spins) are made up almost entirely of Ce 4f states. The contribution of the Ce 4f orbitals to the other occupied states is almost zero. In contrast with this, the Ce 5d orbitals—though appearing mostly in the unoccupied set of states between 2 and 4 eV—are mixed more strongly into occupied states. Still, the largest contributors by far to the occupied states below -2 eV are the Br 4p orbitals (this projection is not shown in Figure 4). The COHP curves of Figure 4 reveal that the occupied, primarily Br 4p, states below -2 eV are Ce–Br bonding and practically Ce–Ce nonbonding, as expected. The occupied, primarily Ce 4f, states in the vicinity of ε_F contribute little to either the Ce–Br or Ce–Ce COHPs. The integrated Ce–Br COHP is -4.72 eV, which breaks down to –0.55 eV per bond for each of the six bonds within the chain (3.11 Å) and -0.48 eV per bond for each of the three face-capping bonds (3.16 Å). The integrated Ce–Ce COHP is -0.01 eV (-0.005 eV per bond); this is essentially nonbonding.

Finally in Figure 5 we present a contour plot of the electron density of $CeBr_3$, evaluated in a plane perpendicular to the c axis containing the Ce atoms. On the left side of Figure 5, the electron density associated with the bonds between Ce and the face-capping Br atoms is clearly visible. The energy slice on the right side of Figure 5 further demonstrates the spatial localization of the Ce 4f levels mentioned above. Even though we are plotting very low electron-density levels, the contours in this plot are still quite close to the Ce nuclei.

Calculations were also carried out on the Ce^{3+} compounds CeF_3 and $CeCl_3$. $CeCl_3$ crystallizes in the same structure type as $CeBr_3$,[21] while CeF_3 is found in a different structure[22] (not

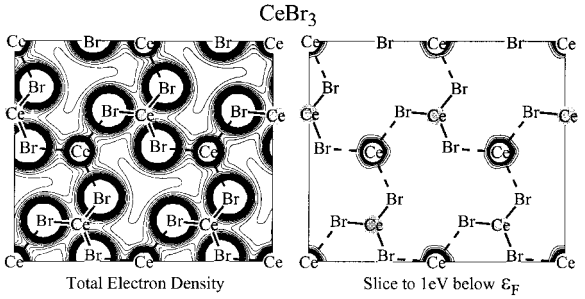

Figure 5. Contour plots of the total electron density (left) of $CeBr_3$ and an energy slice containing only the levels between ε_F and 1 eV below ε_F (right). Ce atoms in shaded circles are not in the same plane, but are included to make the connection to the full structure (shown in Figure 1) clearer. 20 contours equally spaced between 0 and 0.05 electrons a_0^{-3} (where a_0, the Bohr radius, is about 0.529 Å) are shown.

discussed here). The qualitative trends within this series of similar compounds are what we would expect: as the electronegativity of X in CeX_3 increases, the contributions of Ce to occupied orbitals decreases. In all three compounds the Ce 5d AOs play an important role in the bonding, an unexpected result for Ce^{3+}. While CeN also formally contains Ce^{3+}, because it is somewhat special it will be examined in detail in its own section below, after a treatment of some Ce^{4+} compounds.

Tetravalent cerium: The Ce^{4+} compound we choose to focus detailed attention upon is CeO_2. CeO_2 crystallizes in the fluorite (CaF_2) structure type, shown in Figure 6. Each Ce atom is surrounded by eight oxygens at a distance of 2.34 Å.[23]

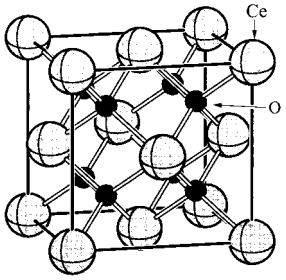

Figure 6. A view of the crystal structure of CeO_2.

The shortest distance between Ce^{4+} ions, within their face-centered cubic (fcc) arrangement is 3.83 Å of which there are twelve. This is quite a bit longer than the sum of the ionic radii (1.94 Å for 8-coordinate Ce^{4+})[19, 20]. As we would expect for a Ce^{4+} compound, CeO_2 shows no tendency to enter a spin-polarized state. Calculations started in a spin-polarized configuration always return to a nonpolarized (all spins paired) state.

Following the same development as for $CeBr_3$, the band structure of CeO_2, along with fatband projections for the Ce 4f and 5d orbitals, is shown in Figure 7. Here the primarily Ce 4f states are clearly unoccupied, lying between 2 and 4 eV above ε_F at the top of the gap. They make only small contributions to the occupied bands within the one eV range immediately below ε_F. Once again the Ce 5d orbitals are

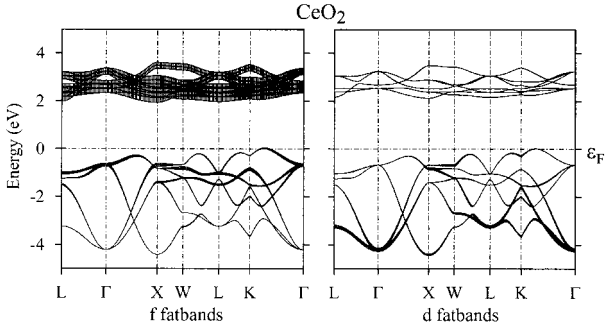

Figure 7. Fatband plots for CeO_2. The widths of the lines are proportional to the contribution of the Ce 4f (left plot) or Ce 5d (right plot) atomic orbitals to the crystal orbitals. The bands are shifted so that ε_F (indicated with a horizontal dotted line) lies at 0 eV.

mixed into occupied bands, making small contributions to the bands around -4 eV.

The projected DOS curves for the Ce orbitals, along with Ce–O and Ce–Ce COHP curves, are shown in Figure 8. The projected DOS curves here support our earlier statement that the states above the gap (the peak in the DOS between 2 and 4 eV) are primarily Ce 4f in character. The peak between 0 and -4 eV is primarily composed of O 2p states (projection not shown here) with a small admixture of the Ce 4f orbitals towards the top and contributions from the Ce 5d orbitals throughout.

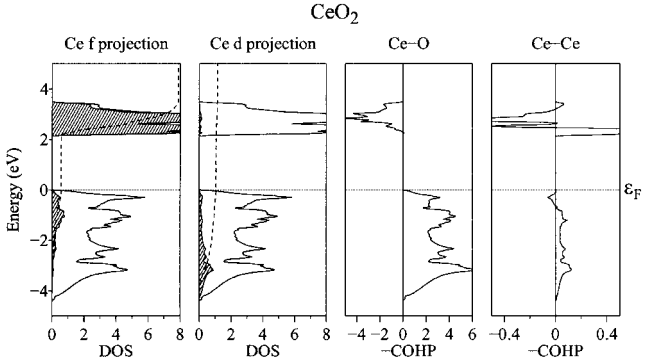

Figure 8. Total DOS, Ce 4f and 5d projected DOSs, and COHP curves for the Ce–O and Ce–Ce interactions in CeO_2. The dashed line in each DOS curve shows the integration of the projected states. To make the projected DOS curves more visible, the DOS is magnified. The Ce–O COHP includes the sum of all eight close Ce–O contacts, while the Ce–Ce curve is the sum of the twelve 3.83 Å Ce–Ce contacts. All curves are shifted so that ε_F (the horizontal dotted line) lies at 0 eV.

The COHP curves of Figure 8 reveal, unsurprisingly, that the peak in the DOS between 0 and -4 eV is Ce–O bonding. The integrated Ce–O COHP is -12.18 eV, giving -1.52 eV per Ce–O bond. The Ce–Ce interactions are stronger than those in $CeBr_3$ (the Ce–Ce COHP plots of Figures 4 and 8 are on the same horizontal scale), but are still very weak. The integrated Ce–Ce COHP is only -0.12 eV, or -0.01 eV per Ce–Ce contact. The partially occupied Ce orbitals are more strongly involved in Ce–O bonds than in interactions between Ce atoms, as we would expect.

A contour plot of the total electron density is presented in Figure 9. The electron density in the regions corresponding to

0947-6539/99/0502-0518 $ 17.50+.50/0 *Chem. Eur. J.* **1999**, *5*, No. 2

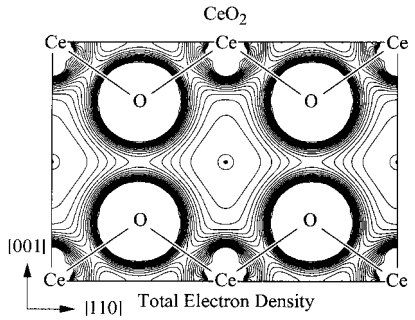

Figure 9. Contour plot of the total electron density of CeO_2. The plane selected, defined by the [110] and [001] axes, contains all of the labeled atoms. 20 contours equally spaced between 0 and 0.05 electrons a_0^{-3} are shown.

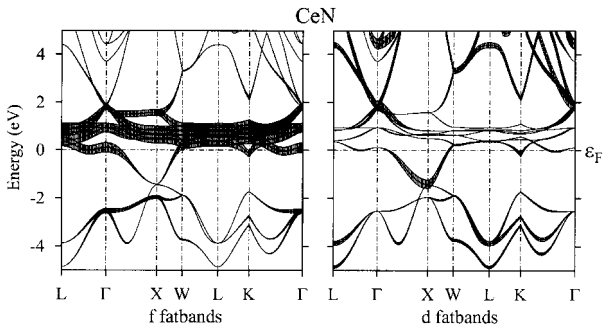

Figure 10. Fatband plots for CeN. The widths of the lines are proportional to the contribution of the Ce 4f (left plot) or Ce 5d (right plot) atomic orbitals to the crystal orbitals. The bands are shifted so that ε_F (indicated with a horizontal dotted line) lies at 0 eV.

Ce–O bonds is easily visible, as is the lack of any significant accumulation of electron density between the Ce^{4+} ions.

We also studied the electronic structures of CeC, Li_2CeN_2, and Li_2CeP_2. CeC crystallizes in the NaCl structure type,[24] while Li_2CeN_2 and Li_2CeP_2 are found in the La_2O_3 structure type.[25, 26] It is more difficult to say anything about expected qualitative trends within this series of compounds because there is little which relates them to each other. Once again, however, the Ce 5d orbitals play an important role in the bonding.

Cerium Nitride: Cerium nitride (CeN) is a fascinating compound. Since CeN is found in the NaCl structure type, it is likely to contain Ce^{3+} and N^{3-} ions (i.e., there are no N–N bonds that would lower the oxidation state on the N). It is, however, a conductor. This leads to the possibility of a crystal composition of the form $Ce^{4+}N^{3-} \cdot e^-$, with one electron left in the conduction band (this is an argument which has been used to understand the high-pressure iso-structural phase transition of SmS[27]).

The magnetic properties of CeN are those one would expect of a conductor: Pauli paramagnetism is observed, which is definitely out of the ordinary for a Ce^{3+} compound. The other Ce pnictides (CeP, CeAs, CeSb, and CeBi), which also appear in the NaCl structure, show more conventional behavior, that is, antiferromagnetic ordering of the 4f electron remaining on each Ce.[28] The reasons for the peculiar electronic and magnetic properties of CeN have been extensively debated in the literature. The most prevalent explanations are mixed valency of Ce,[2, 29] in which Ce can behave as either Ce^{3+} or Ce^{4+}, and itinerant 4f electrons,[30] in which the Ce 4f orbitals are involved in Ce–Ce bonding.

We will not spend time here on a detailed examination of the differences between CeN and the other Ce pnictides. We wish merely to understand the bonding in a compound which, though probably containing Ce^{3+}, does not have a magnetic moment (unpaired electrons) on Ce. Spin-polarized calculations on CeN show the same behavior as those for the Ce^{4+} compounds discussed earlier; the electrons in CeN do not want to be unpaired.

Beginning our analysis as before, Figure 10 shows a fatband plot for CeN. The Ce 4f levels are clearly highly localized in energy (indicating spatial localization, as discussed before), just as they were in $CeBr_3$ (Figure 3). The largest difference between CeN and $CeBr_3$ is that in CeN the primarily 4f states lie *above* ε_F; they are not occupied. Again the admixture of Ce 4f orbitals into states below ε_F is quite small. The behavior of the Ce 5d orbitals in CeN is, however, completely different from that in $CeBr_3$. The occupied band immediately below ε_F (clearly visible along the symmetry lines $\Gamma \rightarrow X \rightarrow W$), which carries the remaining Ce-centered electron, has quite a large contribution from the Ce 5d orbitals.

The COHP curves for CeN, Figure 11, show that the states just below ε_F (between 0 and -2 eV) contain strong Ce–Ce interactions, while contributing almost nothing to the Ce–N bonding. Indeed, the integrated Ce–Ce COHP is -1.14 eV, or -0.10 eV for each of the twelve 3.57 Å Ce–Ce contacts. This is one sixth of the value in fcc Ce, in which each of the twelve 3.64 Å Ce–Ce bonds contribute -0.59 eV to the integrated Ce–Ce COHP.

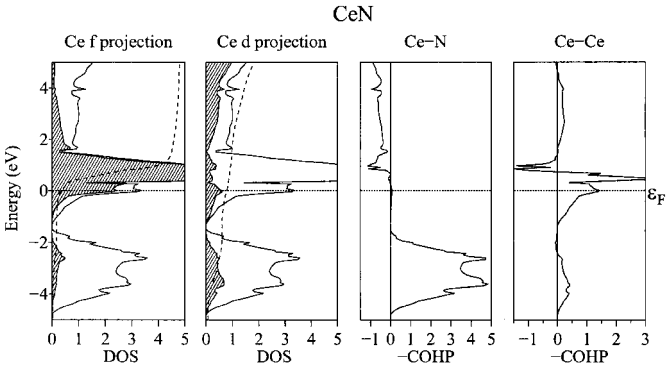

Figure 11. Total DOS, Ce 4f and 5d projected DOSs, and COHP curves for the Ce–N and Ce–Ce interactions in CeN. The dashed line in each DOS curve shows the integration of the projected states. To make the projected DOS curves more visible, the DOS is magnified. The Ce–N COHP includes the sum of all six close Ce–N contacts, while the Ce–Ce curve is the sum of the twelve Ce–Ce contacts. All curves are shifted so that ε_F (the horizontal dotted line) lies at 0 eV.

CeN is a compound in which reliance upon ionic radii can get us into trouble. The Ce–Ce bond length, 3.57 Å, is definitely larger than twice the effective Ce^{3+} ionic radius for twelve coordinate cerium (2.68 Å),[19, 20] leading us to expect no significant Ce^{3+}–Ce^{3+} interactions. It is important to keep in mind that, while the distances between ceriums are long for

Ce^{3+}–Ce^{3+} interactions, they are still about the same length as those in metallic Ce. Ionic radii clearly cannot be used to a priori rule out covalent interactions.

The COHP and band structure results point us towards the reason for CeN's unusual magnetic behavior (or lack thereof). The remaining electron on the Ce^{3+} is found in a spatially diffuse 5d–4f hybrid orbital instead of a highly localized 4f orbital. The spatial extent of the electrons in the band just below ε_F can be quite clearly seen in a plot of a energy slice through the electron density of CeN, Figure 12. In contrast to

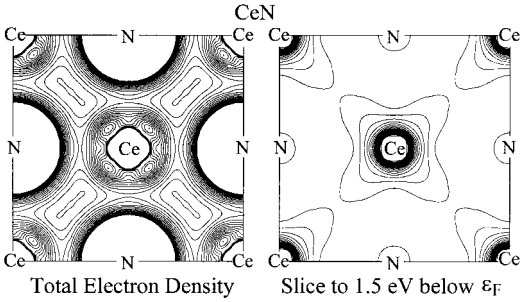

Figure 12. Contour plots of the total electron density (left) of CeN and an energy slice containing only the levels between ε_F and approximately 1.5 eV below ε_F (right). 20 contours equally spaced between 0 and 0.05 electrons a_0^{-3} are shown.

the energy slice for $CeBr_3$ in Figure 9, the states just under ε_F in CeN are delocalized along the directions of the Ce–Ce interactions. Another way of saying the same thing is that the remaining electron on the Ce^{3+} is localized in a Ce–Ce bond instead of being localized on the ion itself. We note that this electron is certainly associated with the Ce centers, not delocalized in some free-electron-like band. This rules out the crystal composition $Ce^{4+}N^{3-}\cdot e^-$ mentioned above.

All of the results for CeN point in the same direction: the lack of spin polarization is due to interactions between the Ce^{3+} centers, which causes occupation of Ce 5d orbitals instead of the 4f orbitals we would expect to be occupied in Ce^{3+}. The valence electron configuration of Ce in CeN is perhaps best described as somewhere in between $(4f)^0(5d)^1(6s)^0(6p)^0$ and $(4f)^1(5d)^0(6s)^0(6p)^0$.

Our conclusions about the importance of Ce–Ce interactions in CeN are in line with recently reported analyses of the electronic structures of both CeN[30] and metallic Ce itself.[31, 32] These studies, based upon the full-potential LMTO method, all indicate that Ce–Ce interactions are very important in these systems. Recent experimental studies of another Ce^{3+} compound, $CeRh_3B_2$,[33, 34] show that Ce 5d orbitals can play a major role in both bonding and magnetic properties.

Preliminary results of a theoretical experiment in which the Ce–Ce interactions in CeN are weakened by increasing the lattice constant (a situation which is, unfortunately, not easily experimentally realizable) indicate that, after a point, the remaining electron on Ce^{3+} moves from the 5d to the 4f orbital, and the expected spin-polarization is favored. These results, along with further analysis of the interactions in CeN and the other Ce pnictides, will be presented elsewhere.

Ce_2MnN_3: The preparation, crystal structure, and magnetic and transport properties of Ce_2MnN_3 were reported in ref. [1]. A possible crystal composition would be $(Ce^{3+})_2Mn^{3+}(N^{3-})_3$, but the alternative $(Ce^{4+})_2Mn^{+}(N^{3-})_3$ is also possible. Both notions would be in harmony with the experimental finding of a practically nonmagnetic material with only a very small (probably impurity-induced) residual effective moment of about 0.53 μ_B, since both low-spin Mn^{3+} and low-spin Mn^+ do not exhibit any spin magnetism. The preceding discussion also makes it clear that the lack of magnetic properties does not offer a clue in distinguishing trivalent and tetravalent Ce, especially when they appear in a metallic compounds such as Ce_2MnN_3. Can theory help in this particularly case?

One view of the structure of Ce_2MnN_3 is shown in Figure 13. In ref. [1] the Mn–N bonding in the one dimensional MnN_3 chains of Ce_2MnN_3 was analyzed in detail. Here we focus on the bonding around the Ce atoms. The

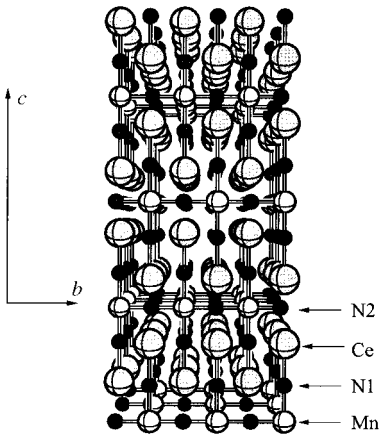

Figure 13. A view of the structure of Ce_2MnN_3 down the *a* axis.

coordination environment of Ce in Ce_2MnN_3 is shown in **1**. There are seven close Ce–Ce contacts (recall that the Ce–Ce distance in fcc Ce is 3.64 Å), as well as Ce–N and Ce–Mn contacts, that are potentially important.

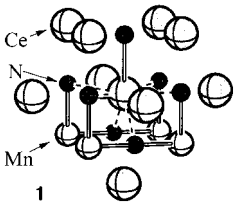

1

Ce-N:	2.36 x1
	2.52 x2
	2.55 x4
Ce-Mn:	3.13 x4
Ce-Ce:	3.44 x2
	3.62 x4
	3.65 x1

A spin-polarized calculation on Ce_2MnN_3 yields results that are in agreement with the experimental data: Ce_2MnN_3 is metallic and there is no tendency whatsoever for a residual magnetic moment at either Ce or Mn. While this points towards assignment of an oxidation state of Ce^{4+}, it is not conclusive, as the discussion of CeN made it clear that it is possible for a Ce^{3+} compound with close Ce–Ce contacts to favor a spin-unpolarized state through formation of Ce–Ce bonds.

Once again we start our analysis of the bonding with fatband plots in the vicinity of ε_F for Ce_2MnN_3 (Figure 14). This plot contains far more bands than we have seen thus far

0947-6539/99/0502-0520 $ 17.50+.50/0 *Chem. Eur. J.* **1999**, *5*, No. 2

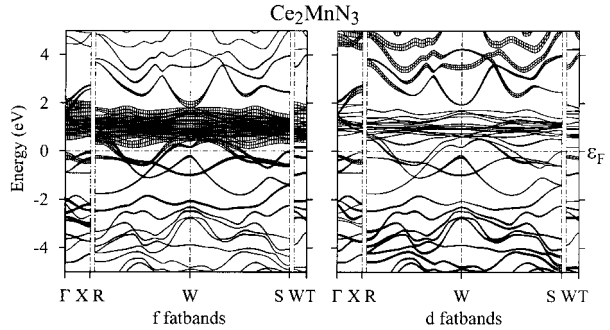

Figure 14. Fatband plots for Ce_2MnN_3. The widths of the lines are proportional to the contribution of the Ce 4f (left plot) or Ce 5d (right plot) atomic orbitals to the crystal orbitals. The bands are shifted so that ε_F (indicated with a horizontal dotted line) lies at 0 eV.

(it is truly a spaghetti diagram). The presence of Mn 3d levels in the immediate vicinity of ε_F (this was discussed in the earlier work) complicates the picture somewhat, but if we try to only focus on the bands which have significant Ce contributions, we see a picture which is closer to CeO_2 (Figure 7 without the large gap of course) than CeN (Figure 10). While there are small admixtures of both Ce 4f and 5d orbitals into the occupied states around ε_F, we do not observe a band with large Ce 5d contribution, like that present in CeN. The lack of a set of occupied states that are largely Ce 5d in character leads us towards an assignment of Ce^{4+}. Trivalent Ce without significant Ce–Ce interactions (which are mediated through 5d–5d interactions) is just too likely to be magnetic.

The Ce–Ce COHP curve, shown in Figure 15, supports our idea that the Ce–Ce interactions in Ce_2MnN_3 are weak. While there are certainly visible interactions between the Ce atoms, the scale of the Ce–Ce COHP curve is only one sixth (!) of

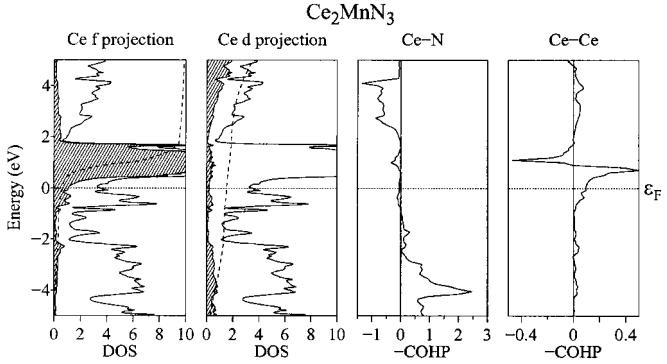

Figure 15. Total DOS, Ce 4f and 5d projected DOSs, and COHP curves for the Ce–N and Ce–Ce interactiosn in Ce_2MnN_3. The dashed line in each DOS curve shows the integration of the projected states. To make the projected DOS curves more visible, the DOS is magnified. The Ce–N COHP includes the closest Ce–N contacts and the Ce–Ce curve is the sum of all seven close Ce–Ce contacts. All curves are shifted so that ε_F (the horizontal dotted line) lies at 0 eV.

that in Figure 11. The states immediately below ε_F that contain reasonably sized contributions from Ce 4f and 5d orbitals, contributing very little to the Ce–N interactions, are involved in the weak Ce–Mn bonding (the Ce–Mn COHP curve, not shown in Figure 15, integrates to only -0.06 eV per bond).

The electron density of Ce_2MnN_3 is shown in Figure 16. The regions corresponding to the Mn–N1 bonds (discussed in ref. [1]) in Figure 16 are devoid of contours because of the high electron density associated with those bonds. The contours chosen (the same as in all other electron density plots in this paper) have small values so as to bring out the detail in the regions around the cerium ions. We can clearly see the electron density corresponding to the bonding interactions between Ce and N1 and N2.

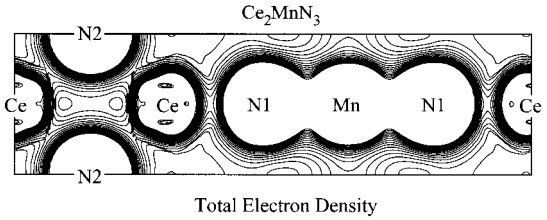

Figure 16. Contour plot of the total electron density of Ce_2MnN_3. 20 contours equally spaced between 0 and 0.05 electrons a_0^{-3} are shown.

Conclusions

While there are significant differences in electronic structure between the members of each class of model compounds (those containing Ce^{3+} and those containing Ce^{4+}), it is still possible to identify the oxidation state of Ce by the use of fatband plots, projected densities of states, and theoretical charge densities. In all of the Ce^{3+} compounds, the Fermi level falls in a region that is primarily made up of Ce orbitals. These may be either very contracted Ce 4f states (e.g., $CeBr_3$, Figure 3), in which case the compound is likely to be paramagnetic, or a mixture of more delocalized Ce 4f and 5d orbitals (e.g., CeN, Figure 10), in which Ce–Ce bonding interactions preclude formation of a magnetic moment. In the Ce^{4+} compounds, the primarily Ce-centered states lie above ε_F, with the only occupation of Ce orbitals arising through covalent interactions. Based upon this criterion, as well as inspection of electron density plots and COHP analysis, we feel comfortable assigning an oxidation state of $+4$ to the Ce in Ce_2MnN_3.

This high Ce oxidation state, which seems unusual in combination with Mn^+ based upon a comparison of E^0 values in aqueous solution, is likely stabilized in the crystal by the coordination environment of the Ce. The strong electrostatic interactions arising from the seven close Ce^{4+}–N^{3-} contacts are even further enhanced by the covalent interactions between cerium and nitrogen.

Acknowledgements

We thank Prof. Shinichi Kikkawa and Prof. Hisanori Yamane for fruitful discussions, and gratefully acknowledge financial support from the New Energy and Industrial Technology Development Organization (NEDO, Japan) under Project Grant MB2: Advanced Nitrides: Novel Approaches, Electrical and Magnetic Properties, and Related Theoretical Calculations.

[1] R. Niewa, G. V. Vajenine, F. J. DiSalvo, H. Luo, W. B. Yelon, *Z. Naturforsch. B* **1998**, *53*, 1.
[2] G. L. Olcese, *J. Phys. F: Metal Phys.* **1979**, *9*, 569.
[3] O. K. Andersen, *Phys. Rev. B* **1975**, *12*, 3060.
[4] H. L. Skriver, *The LMTO Method*, Springer, Berlin, **1984**.
[5] O. K. Andersen, in *The Electronic Structure of Complex Systems* (Eds.:P. Phariseau, W. M. Temmerman), Plenum, **1984**.
[6] O. K. Andersen, C. Arcangeli, R. W. Tank, T. Saha-Dasgupta, G. Krier, O. Jepsen, I. Dasgupta, in *Tight-Binding Approach to Computational Materials Science*, number 491 in MRS Symposia Proceedings, MRS, Pittsburgh, **1998**.
[7] J. Korringa, *Physica* **1947**, *13*, 392.
[8] W. Kohn, N. Rostoker, *Phys. Rev.* **1954**, *94*, 1111.
[9] P. Hohenberg, W. Kohn, *Phys. Rev. B* **1964**, *136*, 864.
[10] W. Kohn, L. J. Sham, *Phys. Rev. A* **1965**, *140*, 1133.
[11] U. von Barth, L. Hedin, *J. Phys. C* **1972**, *5*, 1629.
[12] P. E. Blöchl, O. Jepsen, O. K. Andersen, *Phys. Rev. B* **1994**, *49*, 16223.
[13] O. K. Andersen, O. Jepsen, *Phys. Rev. Lett.* **1984**, *53*, 2571.
[14] G. Krier, O. Jepsen, A. Burkhardt, O. K. Andersen, *TB-LMTO-ASA* program, version 4. 7.
[15] R. Dronskowski, P. E. Blöchl, *J. Phys. Chem.* **1993**, *97*, 8617.
[16] T. Hughbanks, R. Hoffmann, *J. Am. Chem. Soc.* **1983**, *105*, 3528.
[17] R. Hoffmann, *Solids and Surfaces: A Chemist's View of Bonding in Extended Structures*, VCH, Weinheim, **1988**.
[18] W. H. Zachariasen, *Acta Crystallogr.* **1948**, *1*, 265.
[19] R. D. Shannon, C. T. Prewitt, *Acta Crystallogr. B* **1969**, *25*, 925.
[20] R. D. Shannon, *Acta Crystallogr. A* **1976**, *32*, 751.
[21] T. Kojima, T. Inoue, T. Ishiyama, *J. Electrochem. Soc. Japan* **1951**, *19*, 383.
[22] A. K. Cheetham, B. E. F. Fender, H. Fuess, A. F. Wright, *Acta Crystallogr. B* **1976**, *32*, 94.
[23] H. J. Whitfield, D. Roman, A. R. Palmer, *J. Inorg. Nuc. Chem.* **1966**, *28*, 2817.
[24] P. Stecher, A. Neckel, F. Benesowski, H. Nowotny, *Planseeber. Pulvermetall.* **1964**, *12*, 181.
[25] D. Halot, J. Flahaut, *C. R. Hebd. Seances Acad. Sci. Ser. C* **1971**, *272*, 465.
[26] A. E. Maslout, J. P. Motte, A. Courtois, C. Gleitzer, *C. R. Hebd. Seances Acad. Sci. Ser. C* **1975**, *280*, 21.
[27] N. N. Greenwood, A. Earnshaw, *Chemistry of the Elements*, Pergamon, New York, **1984**.
[28] For a recent comprehensive theoretical study of the magnetic properties of the Ce pnictides under pressure, see: A. Svane, Z. Szotek, W. M. Temmerman, H. Winter, *Solid. State Commun.* **1997**, *102*, 473.
[29] H. Bartholin, D. Florence, G. Parisot, J. Paureau, O. Vogt, *Phys. Lett. A* **1977**, *60*, 47.
[30] A. Delin, P. M. Oppeneer, M. S. S. Brooks, T. Kraft, J. M. Wills, B. Johansson, O. Eriksson, *Phys. Rev. B* **1997**, *55*, 10173.
[31] P. Söderlind, O. Eriksson, B. Johansson, J. M. Wills, *Phys. Rev. B* **1995**, *52*, 13169.
[32] P. Ravindran, L. Nordström, R. Ahuja, J. M. Wills, B. Johansson, O. Eriksson, *Phys. Rev. B* **1998**, *57*, 2091.
[33] K. Yamaguchi, H. Namatame, A. Fujimori, T. Koide, T. Shidara, M. Nakamura, A. Misu, H. Fukutani, M. Yuri, M. Kasaya, H. Suzuki, T. Kasuya, *Phys. Rev. B* **1995**, *51*, 13952.
[34] A. Yaouanc, P. Dalmas de Réotier, J. P. Sanchez, T. Tschentscher, P. Lejay, *Phys. Rev. B* **1998**, *57*, 681.

Received: August 12, 1998 [F1304]

  0947-6539/99/0502-0522 $ 17.50+.50/0